Structural transitions in the synaptic SNARE complex during Ca^{2+}-triggered exocytosis

Xue Han and Meyer B. Jackson

Department of Physiology, University of Wisconsin Medical School, Madison, WI 53706

The synaptic SNARE complex is a highly stable four-helix bundle that links the vesicle and plasma membranes and plays an essential role in the Ca^{2+}-triggered release of neurotransmitters and hormones. An understanding has yet to be achieved of how this complex assembles and undergoes structural transitions during exocytosis. To investigate this question, we have mutated residues within the hydrophobic core of the SNARE complex along the entire length of all four chains and examined the consequences using amperometry to measure fusion pore opening and dilation. Mutations throughout the SNARE complex reduced two distinct rate processes before fusion pore opening to different degrees. These results suggest that two distinct, fully assembled conformations of the SNARE complex drive transitions leading to open fusion pores. In contrast, a smaller number of mutations that were scattered through the SNARE complex but were somewhat concentrated in the membrane-distal half stabilized open fusion pores. These results suggest that a structural transition within a partially disassembled complex drives the dilation of open fusion pores. The dependence of these three rate processes on position within the SNARE complex does not support vectorial SNARE complex zipping during exocytosis.

Introduction

Ca^{2+}-triggered exocytosis depends on the coordinated action of several proteins to guide vesicles through a sequence of steps that begins with the docking of a vesicle to the plasma membrane and culminates with membrane fusion (Jahn and Sudhof, 1999; Lin and Scheller, 2000). Among the most important proteins in this process are the synaptic SNAREs, which are members of a large class of membrane trafficking proteins. The synaptic SNAREs are dedicated to neurotransmitter and hormone release and include syntaxin (Syx), synaptobrevin (Syb), and synaptosome-associated protein of 25 kD (SNAP-25; Sollner et al., 1993b). These three proteins can induce slow fusion when reconstituted into liposomes (Weber et al., 1998; Melia et al., 2002), and this fusion becomes Ca^{2+} sensitive with the inclusion of the Ca^{2+} sensor protein synaptotagmin (Tucker et al., 2004). Clostridial neurotoxins specifically cleave SNARE proteins to inhibit synaptic transmission (Jahn et al., 1995; Schiavo et al., 2000), and these reagents provide some of the most compelling evidence that SNAREs are essential for neurosecretion.

SNAREs engage each other through long α-helical domains, termed SNARE motifs, to form a highly stable complex that is referred to as the SNARE complex (Hayashi et al., 1994; Fasshauer et al., 1998; Poirier et al., 1998). The crystal structure of the heterotrimeric SNARE complex has revealed a parallel four-helical bundle with one helix from Syx, one from Syb, and two from SNAP-25. The core of this bundle comprises layers of mostly hydrophobic amino acid side chains (Sutton et al., 1998). Mutations that disrupt complex formation generally reduced fusion efficiency, supporting the view that the SNARE complex plays an important role in exocytosis (Littleton et al., 1998; Chen et al., 1999; Wei et al., 2000; Fergestad et al., 2001; Finley et al., 2002).

It has been difficult to ascertain when the SNARE complex assembles during exocytosis and whether it forms during an early priming step or a later fusion step. In squid nerve terminals, clostridial neurotoxins and soluble SNARE fragments do not reduce the number of docked vesicles even as they poison synaptic transmission (Augustine et al., 1999). Genetic manipulations of the SNARE proteins generally reduce or block synaptic transmission (Schulze et al., 1995; Schoch et al., 2001; Washbourne et al., 2002) without altering docking (Broadie et al., 1995; Sorensen et al., 2003; Deak et al., 2004), suggesting a role for SNARE proteins after vesicle docking. The Syx transmembrane segment is a structural component of the fusion pore

Correspondence to M. Jackson: mjackson@physiology.wisc.edu

X. Han's present address is Department of Molecular and Cellular Physiology, Stanford University Medical Center, Stanford, CA, 94305.

Abbreviations used in this paper: ANOVA, analysis of variance; PSF, prespike feet; Syb, synaptobrevin; Syx, syntaxin; TM, transmembrane domain.

The online version of this article contains supplemental material.

The Journal of Cell Biology, Vol. 172, No. 2, January 16, 2006 281–293
http://www.jcb.org/cgi/doi/10.1083/jcb.200510012

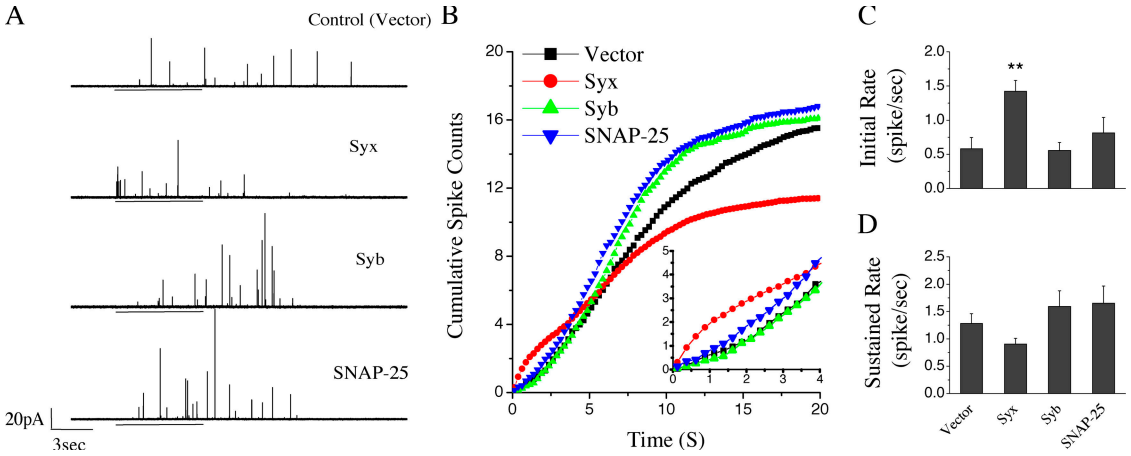

Figure 1. **Overexpressing wild-type SNARE proteins influenced the kinetics of exocytosis.** (A) Amperometry traces from cells overexpressing the synaptic SNARE proteins. KCl depolarization for 6.5 s (solid bars) evoked norepinephrine release; each vesicular release event registered as a spike. (B) Cumulative spike counts plotted versus time after the onset of KCl depolarization. Inset shows the same data with expanded scales to emphasize the differences in initial rates. (C) The initial rate of secretion (spike frequency in the first 2 s) was averaged from 43 to 178 cells. This rate is virtually identical to the initial slope of the cumulative spike count plots in B. Overexpressing Syb and SNAP-25 did not alter the initial rate compared with control cells (vector), but Syx produced a significant increase (**, $P < 0.01$; one-way ANOVA). (D) The sustained rate of secretion (spike frequency between 2.5 and 7.5 s after depolarization onset) was averaged over cells. This rate is virtually identical to the maximum slope of the cumulative spike count plots in B. None of these values differed significantly from the control. Error bars represent SEM.

(Han et al., 2004; Han and Jackson, 2005), and fusion pore stability is altered by manipulations of Syb (Borisovska et al., 2005) and SNAP-25 (Sorensen et al., 2003). These results imply a role for SNARE proteins during the final fusion reaction.

Drawing on the structure of the SNARE complex and its unusual stability, investigators have proposed that it assembles in a vectorial fashion from the membrane-distal portion to the membrane-proximal portion. This "zipping" of the SNARE complex would then perform an essential function in overcoming repulsive forces between the lipid bilayers of the vesicle and plasma membranes (Hanson et al., 1997; Lin and Scheller, 1997; Sutton et al., 1998; Fiebig et al., 1999; Fasshauer, 2003). Clostridial neurotoxins cleave only uncomplexed SNAREs (Hayashi et al., 1994), and their effectiveness in unstimulated chromaffin cells indicates that a large amount of uncomplexed SNARE protein is present in the absence of Ca^{2+} (Xu et al., 1998). At the crayfish neuromuscular junction, botulinum neurotoxin B, which binds to the membrane-proximal region of Syb, also blocked exocytosis without stimulation, but tetanus toxin, which binds to a membrane-distal part of Syb, only inhibited exocytosis after stimulation. These findings led Hua and Charlton (1999) to propose that the SNARE complex partially assembles at the membrane-distal end before Ca^{2+} influx. Additional results showing differential effects in chromaffin cells of antibodies against SNARE proteins also support a partially assembled complex (Xu et al., 1999). However, experiments in permeabilized PC12 cells argue that the SNARE complex assembles after Ca^{2+} addition and before fusion (Chen et al., 1999).

In this study, we attempted to define more precisely what the synaptic SNARE proteins are doing in specific stages of exocytosis. SNARE motif mutants were expressed in PC12 cells, and exocytosis was investigated with carbon fiber amperometry. Kinetic analysis revealed multiple effects of these mutations on kinetic processes both before and after fusion pore opening. These results indicate that the SNARE complex undergoes conformational transitions both to open and then to dilate the fusion pore.

Results

The synaptic SNARE proteins and fusion kinetics

Depolarization of cells transfected with cDNA encoding wild-type synaptic SNARE proteins elicited robust secretion similar to that seen in control cells transfected with vector lacking an insert (Fig. 1 A). The secretion in control cells was ~50% higher than in previous studies from this laboratory (Wang et al., 2001) as a result of modified culture conditions (see Cell culture). Spikes in amperometric current traces signal the exocytosis of single vesicles, and we used the frequency of these spikes as a basic kinetic measure of release. Cumulative spike plots in Fig. 1 B provide a readout of the time course of secretion. In untransfected cells, control cells, and cells overexpressing SNAP-25, Syb (Fig. 1 B), synaptotagmin I, synaptotagmin IV (Wang et al., 2001), NSF, or α-SNAP (Fig. 7), there was a lag of ~2 s before secretion became vigorous. In contrast, cells overexpressing Syx showed an almost immediate response with a lag of only tens of milliseconds and a steep initial slope (Fig. 1 B, inset). The speed of secretion was quantified by measuring the frequency of spikes in the first two seconds of a recording from each cell and then averaging over cells. This initial rate of secretion was virtually identical to the initial slope of the corresponding cumulative spike plots in Fig. 1 B, but by averaging the frequency over cells, we obtained a useful estimate of the error (see Statistics). The initial rate of secretion in cells transfected with Syx cDNA was more than twice as high as in control cells or in cells transfected with Syb or SNAP-25 cDNA, and this difference was highly significant (Fig. 1 C).

After the initial lag, secretion usually reached a maximum rate between 2.5 and 7.5 s. The frequency of spikes in this time interval provided a measure of the sustained rate of secretion, which, when averaged over cells, was virtually identical to the maximum slope of the cumulative spike plots in Fig. 1 B. These rates were roughly similar for cells overexpressing the wild-type SNARE proteins (Fig. 1 D). Syb and SNAP-25 produced small, insignificant increases in the sustained rate, and Syx reduced this rate along with the total number of fusion events (evident in the plateaus in Fig. 1 B). However, the difference between the sustained rates from control and Syx experiments was not significant. The small enhancement with SNAP-25 is consistent with findings in chromaffin cells (Wei et al., 2000). We note that after the KCl depolarization ended at 6.5 s, secretion continued at a steady rate for the duration of the recording in control cells. In contrast, secretion slowed within 4 s after ending the application of depolarizing solution in cells overexpressing any of the SNARE proteins (Fig. 1 B).

SNARE proteins and fusion pores

To assess the effects of SNARE proteins on the stability of the fusion pore, we focused on the foot signal that precedes a spike (Chow et al., 1992). These prespike feet (PSF) reflect catecholamine flux through open fusion pores, and their durations provide a measure of fusion pore stability. PSF duration distributions are generally exponential (Chow et al., 1992; Zhou et al., 1996; Wang et al., 2001) with a time constant equal to the mean PSF duration (Fig. 2, A–D). For cells overexpressing wild-type SNAREs, all mean PSF durations were within 7% of 1 ms, and none of the values differed significantly from the control value (Fig. 2 E). (Note that these values are shorter than the value of 1.38 ms reported previously for the vector control [Wang et al., 2001]. As noted in Cell culture, this change was observed after we started using coated dishes for cell culture). Because PC12 cells express all of these proteins endogenously (Tucker et al., 2003), these results suggest that the stability of fusion pores during exocytosis is not substantially altered by changing the ratios of these proteins. The PSF amplitude also was not altered by overexpressing the different SNARE proteins (see Fig. 8). The constancy of fusion pore properties in the presence of widely varying ratios of SNARE proteins suggests that their actions on open fusion pores depend on a complex with a fixed stoichiometry.

SNARE complex perturbation

To investigate SNARE complex function during exocytosis, we prepared a series of mutations in the hydrophobic core of the SNARE motifs of Syx, Syb, and the NH_2 and COOH chains of SNAP-25 (NH_2 and COOH termini, abbreviated as SNAP-25N and SNAP-25C, respectively). These mutations are illustrated in Fig. 3 and include many double point mutations to alanine in adjacent layers, as in Chen et al. (1999). When alanine was the native residue, it was mutated to leucine, isoleucine, valine, aspartate, or tryptophan. In this study, we refer to mutations by protein/chain and layer according to Sutton et al. (1998). The specifics can be seen in Fig. 3. All of the mutations were intended to reduce the stability of the SNARE complex by either

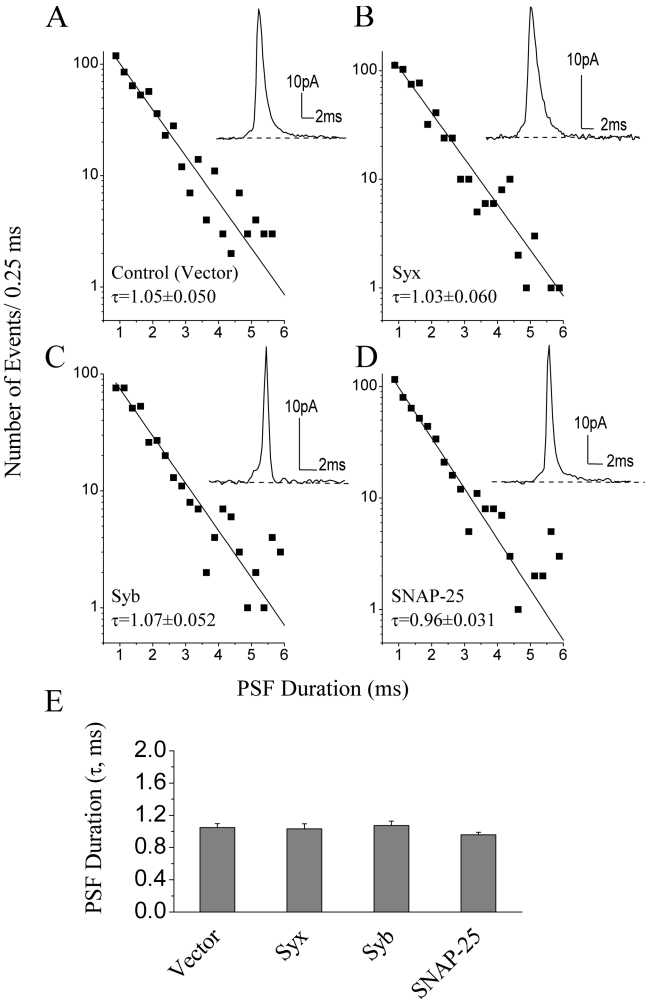

Figure 2. **None of the wild-type SNARE proteins altered the PSF duration.** A representative spike with a PSF is shown in each inset. Event counts per 0.25-ms bin were plotted for control cells (A, vector) and for cells overexpressing Syx (B), Syb (C), and SNAP-25 (D; 407–604 PSF for each plot). Lifetime distributions were well fitted by exponentials (solid lines). The time constant (τ) of the exponential provides a measure of the mean PSF duration (E). Control cells and cells overexpressing Syx, Syb, and SNAP-25 had indistinguishable mean PSF durations. Error bars represent SEM.

creating holes (replacing large side chains by alanine) or by introducing bulk to disrupt packing or charge to favor solvation. Many of our mutations have been characterized previously (Grote et al., 1995; Rossi et al., 1997) and subjected to stability analysis (Hao et al., 1997; Littleton et al., 1998; Chen et al., 1999; Fergestad et al., 2001).

Previous voltage clamp measurements had shown that mutations in the Syx membrane anchor had no effect on Ca^{2+} channels (Han et al., 2004). For this study, we measured Ca^{2+} current in PC12 cells for two Syx mutants (layers −4/−3 and +4/+5), two SNAP-25 mutants (NH_2-chain layer +2/+3 and COOH-chain layer −1/−2), and one Syb mutant (layer +3/+4) along with the wild-type proteins. Mean peak Ca^{2+} currents ranged from −59.5 to −66.9 pA and were indistinguishable from controls (Fig. S1, available at http://www.jcb.org/cgi/content/full/jcb.200510012/DC1). The Syx layer +4/+5 mutant has been implicated in the modulation of heterologously expressed

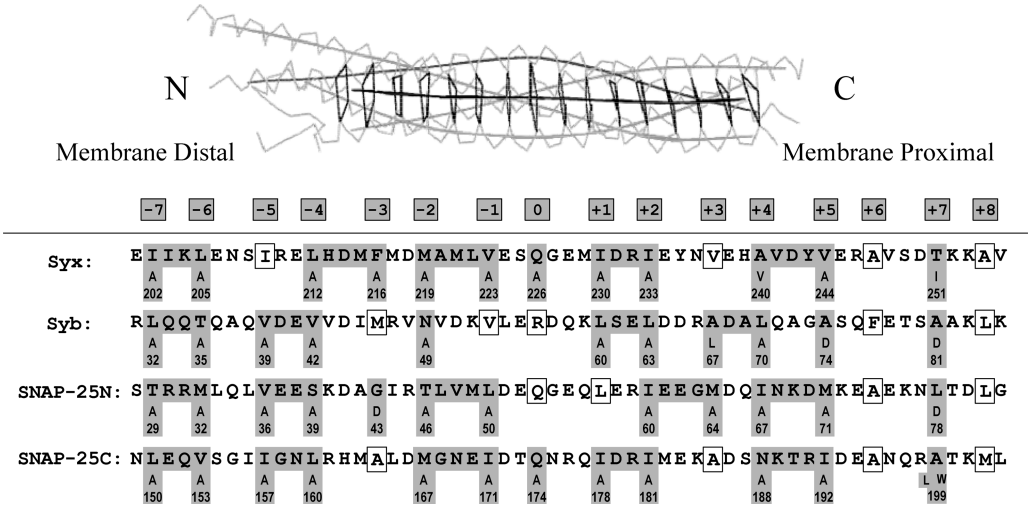

Figure 3. **Mutations in the core of the SNARE complex.** The mutations studied here are indicated in a model of the SNARE complex (Sutton et al., 1998). NH_2 (N) and COOH (C) termini are indicated; the membrane anchors of Syx and Syb are at the COOH termini. Layers −7 to +8 of the central interface are aligned for Syx, Syb, and the NH_2 and COOH chains of SNAP-25 (GenBank/EMBL/DDBJ accession no. P32851, NP_036795, and AAA61741, respectively). Layers tested are highlighted in gray with residues and positions indicated. Untested layers are indicated by open boxes. In layer +7 of SNAP-25C, two different point mutations (with L and W) were studied.

Ca^{2+} channels (Bezprozvanny et al., 2000), but no effects on endogenous Ca^{2+} channels were seen with this mutant. The following two sections show that the mutants we tested have strong effects on exocytosis, and the failure of these mutants to alter Ca^{2+} channels indicates that these mutants are altering exocytosis directly. These mutants, together with wild-type proteins, were also examined by immunocytochemistry to evaluate expression and localization (Fig. S2). Syx and SNAP-25 clearly were localized to the edges of cells, which is consistent with a plasma membrane location. Syb showed a punctal appearance and colocalized with another vesicle protein, synaptotagmin. Mutant SNAREs showed the same localization as the overexpressed wild-type proteins.

SNARE complex functions in exocytosis

The kinetics of release was studied by measuring the initial and sustained rates in cells expressing these mutants after the analysis of wild-type proteins described above (Fig. 1). Most of the core mutations in either the NH_2 or COOH chain of SNAP-25 reduced secretion (Fig. 4, A and B). All of the SNAP-25N mutations except the layer −7/−6 mutation reduced the initial rate of secretion significantly (Fig. 4 A, top right). Small reductions were seen in the sustained rate of secretion as well, but none of these changes were significant except for the layer −2/−1 mutation, in which the effect was only significant by the less stringent *t* test ($P = 0.02$; Fig. 4 A, bottom right). Most of the SNAP-25C mutations reduced the sustained rate significantly (Fig. 4 B, bottom right), but these mutations only slightly reduced the initial rate (the −5/−4 layer mutation effect was significant by the *t* test; $P = 0.007$; Fig. 4 B, top right). SNAP-25C mutations were effective in reducing secretion along the entire length of the SNARE motif, which is in contrast to the experiments of Chen et al. (1999), in which mutations in the hydrophobic layers followed a trend of stronger rescue of secretion toward the membrane-distal end. Neither leucine nor tryptophan at layer +7 reduced either rate significantly, but only the tryptophan results are plotted in Fig. 4 B. Thus, the NH_2 and COOH chains of SNAP-25 had opposite selectivities in their influences on the initial and sustained rates of secretion.

As with SNAP-25, most mutations in Syb reduced secretion (Fig. 4 C, left). Syb mutations more strongly affected the initial rate (Fig. 4 C, top right) than the sustained rate (Fig. 4 C, bottom right). Most of the changes in the initial rate were statistically significant. The changes in the sustained rate were not, except for the layer +3/+4 mutant.

Mutations in Syx also reduced secretion (Fig. 4 D, left). Like the Syb and SNAP-25N mutations, most of the Syx mutations significantly reduced the initial rate (Fig. 4 D, top right) and had smaller, insignificant effects on the sustained rate (Fig. 4 D, bottom right). The Syx layer −7/−6 mutation reduced the sustained rate by an amount that was significant only by the *t* test ($P = 0.02$). The Syx layer −4/−3 mutation was unique in enhancing the initial rate, and this effect was large and highly significant. The Syx layer 0 mutation reduced the initial rate but enhanced the sustained rate, which is in contrast to the effects of the layer 0 mutation of SNAP-25C, which reduced both rates in parallel.

Two-way analysis of variance (ANOVA) was performed to evaluate changes in the initial and sustained rates produced by mutations within each chain. Syx mutations in the same layer often changed the sustained and initial rates differently, and a strong interaction between mutation and rate was evident ($P = 0.0005$). In contrast, the SNAP-25N, SNAP-25C, and Syb chains showed no significant interactions between the effects of mutations and the effects of rates ($P \geq 0.5$ for all), indicating that mutations at the same layer of these chains produced parallel changes in the initial rate and the sustained rate. As stated in Statistics, for parallel changes, we went on to use two-way

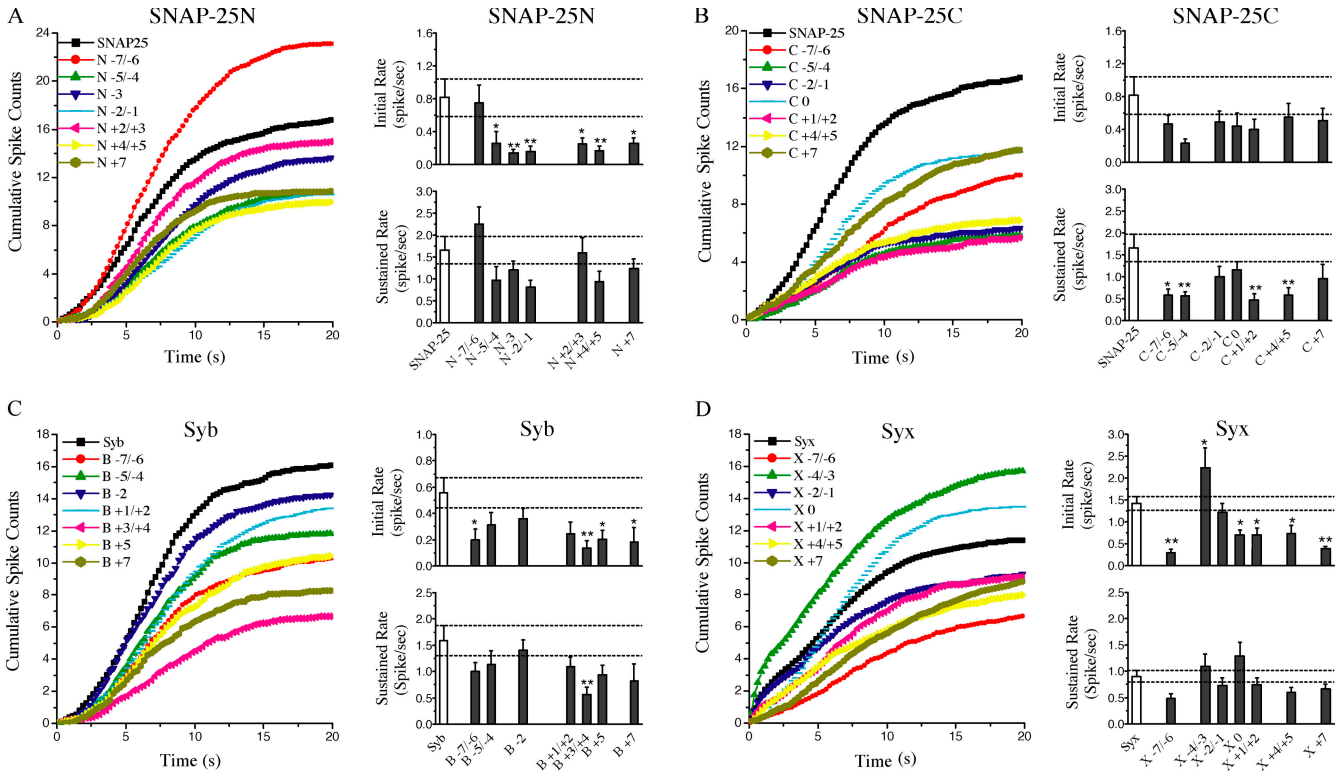

Figure 4. **SNARE complex core mutation effects on secretion kinetics.** SNAP-25N (A), SNAP-25C (B), Syb (C), and Syx (D) with cumulative spike count plots (left) and bar graphs for the rates (right). Wild-type data (Fig. 1) are included for comparison, with dashed lines extending the error bars. The asterisks indicate statistical significance (one-way ANOVA; *, $P < 0.05$; **, $P < 0.01$). (A) SNAP-25N (abbreviated as N) initial rates were reduced significantly by mutations at layers −5/−4, −3, −2/−1, +2/+3, +4/+5, and +7. Sustained rates were apparently lower for most mutants, but the differences were not significant (40–64 cells per measurement). (B) With the SNAP-25 COOH chain (abbreviated as C), initial rates were apparently lower, but the changes were not significant. Sustained rates were reduced significantly by mutations at layers −7/−6, −5/−4, +1/+2, and +4/+5 (28–68 cells per measurement). (C) With Syb (abbreviated as B), initial rates were reduced significantly by mutations at layers −7/−6, +1/+2, +3/+4, +5, and +7. Sustained rates were only reduced significantly by the layer +3/+4 mutation (40–55 cells per measurement). (D) With Syx (abbreviated as X), initial rates were reduced significantly by mutations at layers −7/−6, 0, +1/+2, +4/+5, and +7 and enhanced significantly by the mutation at layer −4/−3. Sustained rates, although lower, were not significantly different (57–178 cells per measurement).

ANOVA to evaluate the contribution of secretion rates and mutations to these changes. These tests indicated that both mutations and rates contributed significantly to the overall variation in measured values ($P < 0.0001$ for each test using all three chains). This analysis confirmed that mutations in Syb, SNAP-25N, and SNAP-25C altered the initial rate and the sustained rate to different degrees.

SNARE complex functions in fusion pores

We next examined the effects of these mutations on PSF to determine how the SNARE complex influences fusion pores. The selected traces show long PSF (Fig. 5 A) and are representative. When SNARE complex mutations altered the PSF duration, it almost always became longer, suggesting these mutations tended to enhance fusion pore stability.

All four chains had some sites where mutations stabilized open fusion pores. However, these sites were limited to certain parts of each chain. In Syx, only mutations in layers −7/−6, −4/−3, and −2/−1 increased PSF duration significantly by one-way ANOVA. The Syx layer +4/+5 and layer +7 mutations had small effects that were only significant by the *t* test ($P = 0.04$ and 0.02, respectively). Syx and Syb mutations with greater effects tended to cluster at the two termini. In SNAP-25N, four mutations in sequence from layer −5 through layer +3 significantly increased the PSF duration. The only mutation that reduced PSF duration anywhere in the SNARE complex was in SNAP-25N at layer −7/−6, and this effect was small (∼15%) but significant. The SNAP-25N layer −7/−6 mutation reduced the PSF duration and increased secretion (Fig. 4 A), and although both changes are opposite to those seen with the majority of mutations (secretion rates generally fell and PSF durations became longer), the changes still showed the same parallel. Mutations in the COOH chain of SNAP-25 that increased the PSF duration fell between layers −7 and +2. However, the layer 0 mutation had no effect. In general, the same layers in the NH_2 and COOH chains of SNAP-25 changed the PSF duration in a similar manner, but this pattern did not extend to Syx and Syb.

In summary, about half of the mutations in the four SNARE chains that we tested influenced the PSF duration. Of the 15 with significant effects, 11 were in negative layers (membrane distal). This contrasts with the more uniform distribution of effects of mutations on the initial and sustained rates. This difference in the dependence on location of mutations indicates that the SNARE complex assumes different conformations during these distinct kinetic steps.

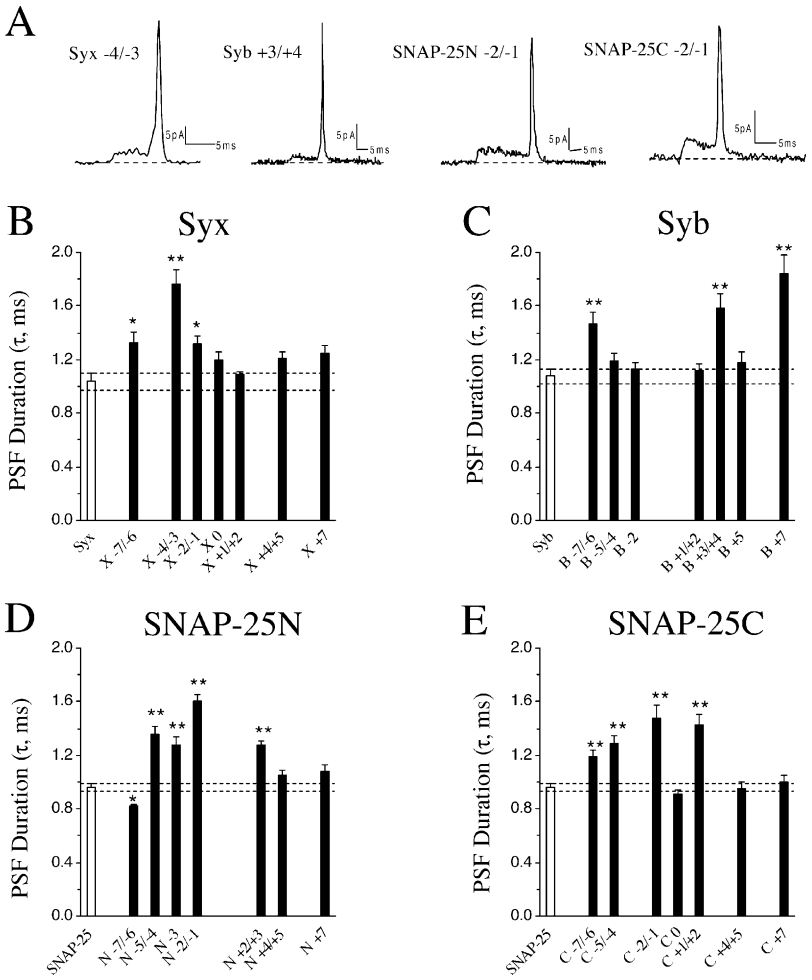

Figure 5. **SNARE complex core mutations influenced fusion pores.** (A) Spikes with long PSF are shown from cells overexpressing the mutant proteins Syx layers −4/−3, Syb layers +3/+4, SNAP-25N layers −2/−1, and SNAP-25C layers −2/−1. Several of the mutations prolonged the foot duration significantly compared with the wild-type proteins. PSF durations were compared for mutations in Syx (B), Syb (C), SNAP-25N (D), and SNAP-25C (E), with wild-type values from Fig. 2 and dotted lines indicating error bars. Event counts were in the ranges 221–559, 211–407, 209–500, and 256–500 for B, C, D, and E, respectively. *, $P < 0.05$; **, $P < 0.01$; from one-way ANOVA.

SNARE complex stability

Many of the mutants tested in this study were previously reported to form SNARE complexes with lower melting temperatures (see supplemental material, available at http://www.jcb.org/cgi/content/full/jcb.200510012/DC1). Other mutants are homologous in design and should also destabilize SNARE complexes. To evaluate our results in terms of SNARE complex stability, we performed linear regression analysis on the initial rate of secretion, the sustained rate of secretion, and PSF duration against the published melting temperatures for wild-type SNAP-25 and seven SNAP-25 mutations (Fig. S3, A–C). No significant correlations were evident. Mutants that destabilize the SNARE complex had varied efficacies in rescuing norepinephrine secretion in PC12 cells (Chen et al., 1999). This lack of correlation with melting temperature suggests that if the complete disassembly that occurs during an in vitro melting experiment is a physiologically relevant transition, it occurs during processes other than those studied here. The changes in the rate processes in exocytosis seen here are more likely to reflect perturbations of other forms of structural transitions in complexes of SNARE proteins.

Syx effects outside the SNARE motif

Overexpressing wild-type Syx accelerated the initial rate of secretion and nearly eliminated the initial lag between depolarization and maximal release (Fig. 1). Because of this remarkable enhancement, additional mutations outside the Syx SNARE motif were tested. Deleting the large NH_2-terminal H_{abc} domain of Syx (ΔH_{abc}) reduced the initial rate significantly compared with wild-type Syx, reducing the rate to a value close to that of control cells (Fig. 6, A and B). Thus, the H_{abc} domain is essential to the initial burst of secretion produced by wild-type Syx. ΔH_{abc} did not alter the sustained rate or the PSF duration (Fig. 6, C and D).

Deleting the Syx transmembrane domain (ΔTM) or increasing the length of the linker between the SNARE motif and the TM (Linker) reduced secretion (Fig. 6 A). Both mutations profoundly reduced the initial rate (Fig. 6 B) and had weaker effects on the sustained rate, but the effect of Linker was significant (Fig. 6 C). These results agree with studies in chromaffin cells (Graham et al., 2004) and liposome fusion assays (McNew et al., 1999). Effects on the PSF duration were small, but the increase in PSF duration produced by linker was significant (Fig. 6 D).

NSF and α-SNAP

The goal of our experiments with SNARE motif mutations was to determine the role of the SNARE complex in secretion. Because NSF and α-SNAP disassemble the SNARE complex (Sollner et al., 1993a; Hayashi et al., 1995), these proteins provide another way to perturb the SNARE complex. Overexpressing

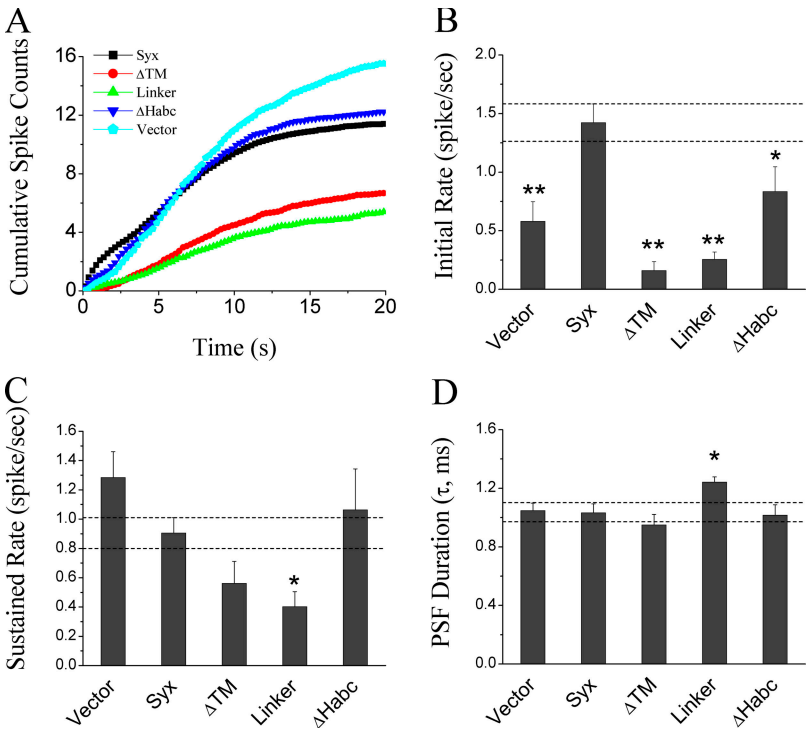

Figure 6. **Syx mutations outside the SNARE complex.** (A) Cumulative spike plots for cells overexpressing the indicated proteins. (B) Initial rates were significantly reduced by deleting the transmembrane domain (ΔTM), lengthening the linker (Linker), or deleting the H_{abc} domain (ΔH_{abc}; 63–178 cells per measurement). There was no difference between the rates for ΔH_{abc} and vector control. (C) The sustained rate was reduced significantly by Linker but not by the other mutants. (D) The PSF duration was not changed by ΔTM or ΔH_{abc} but was increased by Linker (169–559 PSF per measurement; *, $P < 0.05$; **, $P < 0.01$; by one-way ANOVA with wild-type Syx as the control).

these proteins alone or together did not alter secretion rates (Fig. 7). The slight reduction in the initial rate was not significant (Fig. 7 B). The PSF duration was not altered by NSF alone, but α-SNAP either alone or together with NSF increased the PSF duration (Fig. 7 D). This result is consistent with the results of SNARE motif mutations on PSF duration and may also be relevant to the slowing of release at a squid synapse by an NSF peptide (Schweizer et al., 1998). It is notable that two independent methods of perturbing the SNARE complex, overexpressing SNARE mutants and overexpressing NSF/α-SNAP, both stabilized fusion pores.

Fusion pore flux

The Syx transmembrane segment forms the part of the fusion pore through the plasma membrane and contains residues that influence the flux through open fusion pores. Mutations in this region typically alter flux by ∼15%, with changes as high as 23% (Han et al., 2004; Han and Jackson, 2005). Outside of the membrane anchor, mutations throughout the SNARE complex completely failed to alter the PSF amplitude. In these measurements from cells transfected with 39 constructs, PSF amplitude was typically within 5% of control, with the largest change being 10%. One-way ANOVA indicated that none of the values differ significantly (Fig. 8). This demonstrates a striking specificity of influences on fusion pore flux and strengthens our previous conclusion that the Syx membrane anchor forms part of the fusion pore.

Discussion

This study has demonstrated that mutations throughout the SNARE complex influence one or more of the rate processes that are associated with norepinephrine release from PC12 cells. We tested a total of 29 SNARE complex core mutations, which were distributed uniformly through the four chains, and nearly all of them influenced at least one kinetic component of Ca^{2+}-triggered exocytosis. These results indicate that the SNARE proteins are actively involved in transitions on the second time scale before fusion pore opening and the millisecond time scale in open fusion pores. The patterns of effects on the initial rate, the sustained rate, and the fusion pore duration are illustrated in Fig. 9 to aid in the discussion. These figures combine our kinetic results with the crystal structure of Sutton et al. (1998) to illustrate how the same set of mutations produced variable effects on different rate processes. These results support the broad conclusion that the SNARE complex functions in multiple kinetic steps during exocytosis.

Syx in early steps of exocytosis

Syx was unique in enhancing the initial rate of secretion (Fig. 1). The level of endogenous Syx is seven times lower than SNAP-25 in PC12 cells (Tucker et al., 2003). Thus, Syx may be limiting in the initiation of the sequence of events triggered by Ca^{2+}. The Syx H_{abc} domain can fold up with the SNARE motif into an intramolecular four-helix bundle (Dulubova et al., 1999). This "closed" form cannot form SNARE complexes (Pevsner et al., 1994; Misura et al., 2000; Yang et al., 2000) until the SNARE motif dissociates from the H_{abc} domain (Dulubova et al., 1999; Misura et al., 2000). However, deleting H_{abc} removed the initial secretion burst seen with wild-type Syx (Fig. 6, A and B). Thus, the H_{abc} domain apparently does not act as an endogenous inhibitor but has the opposite action in facilitating an early step of release. Because the Syx layer +1/+2 mutation reduces Munc-18 binding (Kee et al., 1995; Wu et al., 1999;

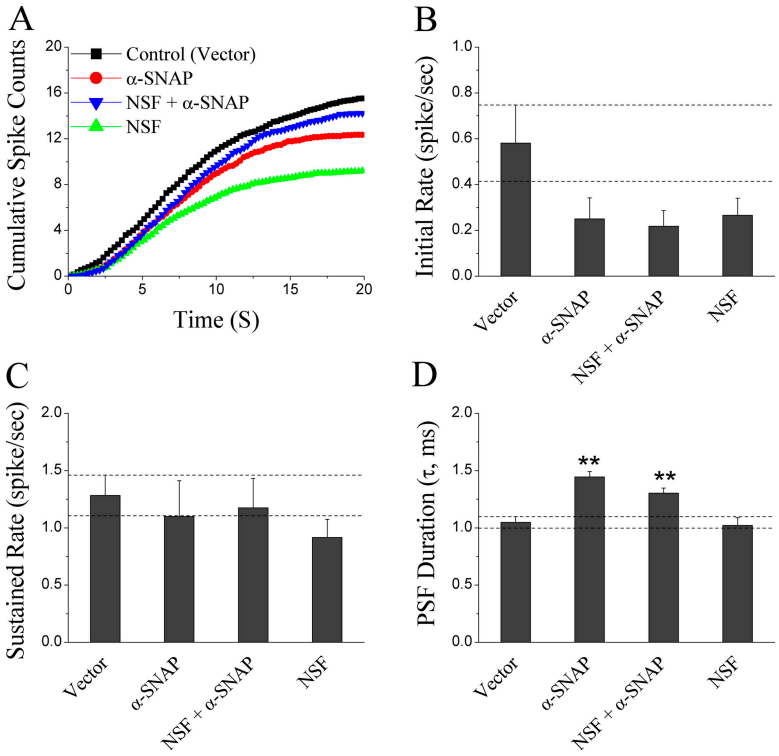

Figure 7. **NSF and α-SNAP effects on exocytosis and fusion pores.** Cumulative spike plots for cells overexpressing NSF, α-SNAP, or both together (A). None of these proteins changed the initial rate (B) or the sustained rate (C) significantly. Overexpressing α-SNAP or NSF + α-SNAP increased the PSF duration significantly (D). α-SNAP had a greater effect on the PSF duration, but there is no significant difference between α-SNAP and NSF + α-SNAP. NSF alone did not change the PSF duration (39–78 cells or 270–604 PSF per measurement; * $P < 0.05$; **, $P < 0.01$; by one-way ANOVA with vector as the control). Error bars represent SEM.

Graham et al., 2004) and Munc-18 promotes formation of the closed form of Syx (Hata et al., 1993; Dulubova et al., 1999; Misura et al., 2000), this mutation should promote the formation of the open form of Syx. Thus, the fact that this mutant reduced secretion is consistent with the idea that the H_{abc} domain does not have an inhibitory role in cells.

The Syx layer −4/−3 mutation had a unique effect, enhancing the initial secretion rate without changing the sustained rate. This was not caused by an alteration of Ca^{2+} current (Fig. S1) and may indicate either that this mutation enhances incorporation into a SNARE complex, enhances a SNARE complex transition, or reduces the binding of another inhibitory protein that has a greater dependence on layers −4/−3.

Multiple SNARE complexes before fusion pore opening

Although the effects of mutations varied quite a bit, mutations in nearly every layer of the SNARE complex inhibited the initial and/or sustained rates of secretion (Fig. 9, A and B). These two kinetic components can be interpreted in terms of models such as those used by Heinemann et. al. (1994) and Lou et al. (2005), in which passage of a fusion complex through a sequence of prefusion states is accelerated by Ca^{2+}. Within such a framework, our initial rate would represent fusion from early states in this sequence (Lou et al., 2005). The sustained rate would represent fusion from later states and, thus, show a lag as these states accumulated in the presence of elevated Ca^{2+}. Alternatively, these two processes could represent parallel pathways leading to the opening of a fusion pore (Voets et al., 1999; Xu et al., 1999). Either way, both the initial and sustained rates represent processes on the pathway leading to fusion pore opening. The finding that mutations throughout the SNARE complex reduced these prefusion pore rates indicates that the SNARE complex assembles before the fusion pore opens.

The SNAP-25N mutations, along with the Syx and Syb mutations, had greater effects on the initial rate, and the SNAP-25C mutations had greater effects on the sustained rate (Fig. 4). These results suggest that these two rate processes have real differences in their structural dependences and, thus, could arise from two distinct, fully assembled SNARE complexes. SNAP-25N, Syx, and Syb may pack loosely in the complex associated with the sustained rate and more tightly in the complex associated with the initial rate. Alternatively, the two SNARE complexes inferred from our results could correspond to those inferred from studies of secretion in chromaffin cells (Voets et al., 1999; Xu et al., 1999). In either scenario, our findings of different profiles of sensitivity in different rate processes give functional relevance to the multiple SNARE complex conformations seen in solution (Fasshauer et al., 2002).

Partial disassembly during fusion pore opening

Syb homologues have been shown to influence fusion pore stability (Borisovska et al., 2005), and this is consistent with the present findings. However, in contrast to rate processes leading to fusion pore opening, the sites that influence the stability of an open fusion pore are scattered through the SNARE complex. Only about half of the mutations tested had a statistically significant effect, and of those the majority (11/15) were in membrane-distal negative layers (Fig. 5). Because the effects on the initial and sustained rates indicated that the SNARE complex is already fully assembled by the time the fusion pore

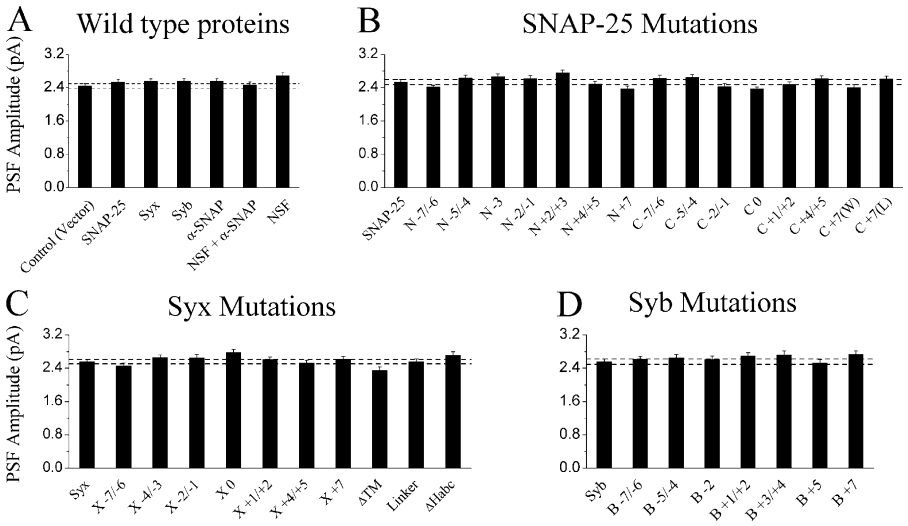

Figure 8. **SNARE mutations failed to alter PSF amplitude.** Wild-type proteins (A), SNAP-25 mutations (B), Syx mutations (C), and Syb mutations (D) produced no significant changes in PSF amplitude by one-way ANOVA. Dashed horizontal lines extend the error bars for the controls or wild-type proteins (far left bars).

opens, the patchy distribution of effects on fusion pore stability may mean that the SNARE complex partially disassembles, either once the fusion pore is open or as it starts to dilate. Reassembly or a structural transition in the membrane-distal regions (which have stronger effects on PSF duration) would then play a critical role in transitions arising from open fusion pores. Overexpression of α-SNAP (alone or with NSF) stabilized open fusion pores (Fig. 7). Because these proteins disassemble the SNARE complex (Sollner et al., 1993a; Hayashi et al., 1995), this result provides another line of evidence in support of the hypothesis of SNARE complex disassembly in open fusion pores. The crystal structure of the SNARE complex is asymmetric, with the two helices of SNAP-25 further apart from the Syx and Syb helices at the COOH terminus (Sutton et al., 1998). The looser packing of the COOH termini of the SNAP-25 helices may be related to the lack of effect of mutations in this region on fusion pore duration.

Syx is a structural component of the fusion pore (Han et al., 2004; Han and Jackson, 2005). A direct physical connection can thus transmit SNARE complex conformational transitions to the fusion pore, with the Syx linker between the SNARE motif and membrane anchor transducing these signals. It is significant that lengthening this linker slowed each of the three rate processes we investigated (Fig. 6). Several proteins have been shown to influence fusion pore properties, including synaptotagmin isoforms (Wang et al., 2001) and phosphatidylinositol phosphate kinase type Iγ (Gong et al., 2005). Mutations in synaptotagmin I that specifically weaken interactions with the SNAREs reduced both fusion pore opening and duration (Bai et al., 2004). Further study of these interactions could clarify the role of SNARE proteins in coupling Ca^{2+} to exocytosis.

An assessment of SNARE complex zipping

We saw no gradient in the efficacy of mutations from the membrane-distal to the membrane-proximal layers of the SNARE motifs in three distinct kinetic steps of exocytosis. Therefore, these results support the notion of SNARE complex formation as a concerted process, as seen in vitro (Zhang et al., 2004), rather than a vectorial process progressing toward the membrane anchors. If SNARE complex zipping were to drive the steps leading to fusion pore opening in sequence, we would expect mutations in the membrane-distal layers to influence the initial and/or sustained rates and mutations in the proximal layers to influence PSF duration. The failure of our data to support this prediction is evidence that the distinct rate processes observed here are not driven by a progressive zipping of the SNARE complex. However, we cannot rule out rapid zipping events within individual rate processes. For example, the initiation of secretion, which is sensitive to mutations in every layer, could proceed through a single zipping transition of the entire complex.

Some prior studies have interpreted experimental results in terms of a zipping model. The differences in use dependence of inhibition by neurotoxins is consistent with this model (Hua and Charlton, 1999), but this observation does not identify the precise time at which a partially assembled state appears during activity. Our data are consistent with a partially assembled SNARE complex after fusion pore opening, but this would still enable activity to expose a cleavage site. We should also point out that PC12 cells are more similar to chromaffin cells, where no use dependence of toxin sensitivity was evident (Xu et al., 1999). In a study with reconstituted proteins, membrane-proximal Syb peptides enhanced SNARE-mediated fusion (Melia et al., 2002). This result was reconciled with a zipping model by postulating that the peptide disrupts an inhibitory interaction while allowing SNARE complexes to assemble. However, this peptide could also stimulate fusion by facilitating the transition to a partially disassembled SNARE complex such as that indicated by our fusion pore data.

A mechanism for SNARE-mediated fusion

To summarize our results, we propose a working model for SNARE-mediated membrane fusion (Fig. 10). An initial assembly step produces the complex shown in Fig. 10 A, and overexpressing Syx can accelerate this step. The initial SNARE complex then rearranges (perhaps with a strengthening of the association with the SNAP-25 COOH chain) to form a closed

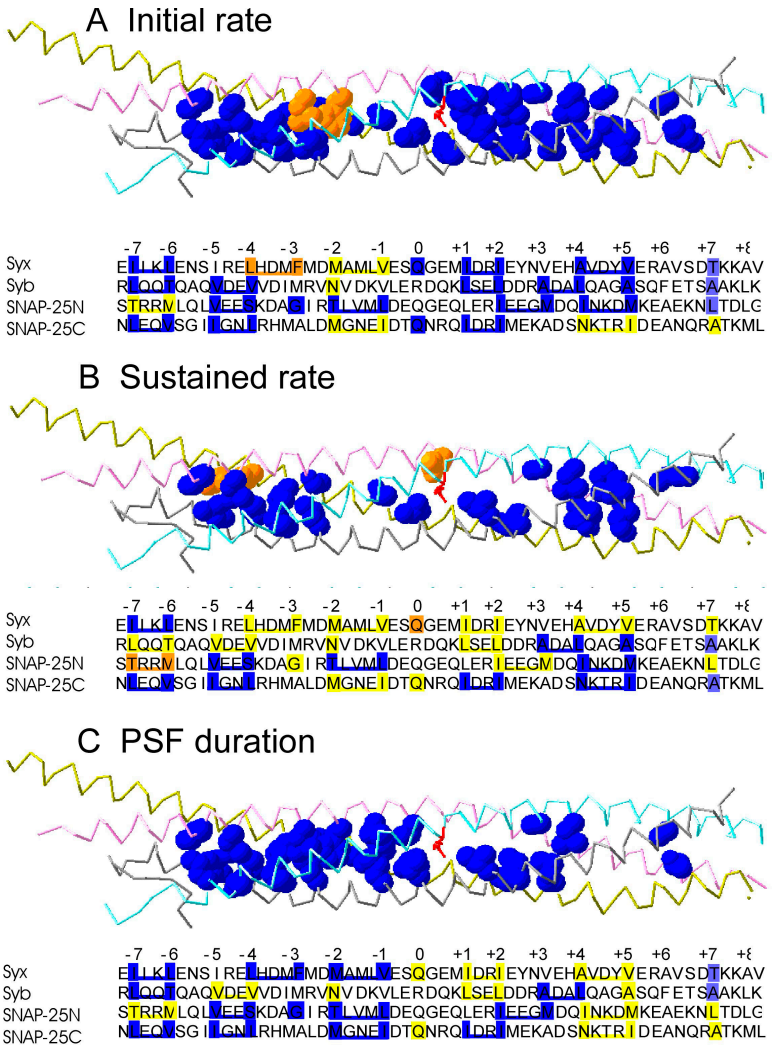

Figure 9. **Summary of kinetic effects of mutations.** The crystal structure of the SNARE complex (Sutton et al., 1998) was used to display the effects of mutations on the initial rate (A), the sustained rate (B), and the PSF duration (C). The backbone chains are displayed for the entire complex (Syx, pink; Syb, light blue; SNAP-25N, olive; SNAP-25C, gray; and Syb layer 0, red). For mutations with an effect, the entire residue is space filling. For the initial and sustained rates, blue indicates >40% decrease, and orange indicates >30% increase. For the PSF duration, blue indicates >20% increase. Below each structural model are sequences with the same color scheme, except that tested mutations with effects below the threshold for blue or orange are shown as yellow.

fusion pore (Fig. 10 B). Transitions from A to B and C (Fig. 10) generate the sustained secretion that follows the initial delay, and the looser SNARE complex in B (Fig. 10) reflects the generally weaker effects of mutations on the sustained rate (except for the COOH chain of SNAP-25). The opening of the fusion pore leads to the configuration in Fig. 10 C, and the partially disassembled SNARE complex shown corresponds roughly with the pattern of sensitivity of the PSF duration to mutations (Figs. 5 and 9 C). Finally, the open fusion pore dilates to state D (Fig. 10), and this transition is driven by some rearrangement and possibly reassembly of the SNARE motifs. We speculate that this reassembly could ultimately lead to a very tight cis complex as the membrane anchors all move to the same membrane. Although the model presents these transitions in a sequence, some branching or steps in parallel before fusion pore opening cannot be ruled out. We mention this because we do not see an inconsistency between our data and the interpretations proposed by Xu et al. (1999) for two SNARE complexes in different states acting in parallel to produce different kinetic components of release.

This study has delineated some of the roles of the synaptic SNARE proteins and their complex in Ca^{2+}-triggered exocytosis. The sensitivities to mutations of various rate parameters, including those related to fusion pore stability, indicate important functions for the SNARE complex in kinetic processes underlying exocytosis. Insights such as these hold promise in the development of a detailed molecular model for secretion. Among the important questions that remain is how the signal of Ca^{2+} binding to its sensor protein synaptotagmin triggers exocytosis. Mapping out binding sites of SNARE-binding proteins and using mutagenesis in a functional assay such as that used here should illuminate the roles of various signaling proteins in initiating and regulating the functional transitions of the SNARE complex brought to light in this study.

Materials and methods

Amperometry

Norepinephrine release was recorded with a VA-10 amperometry amplifier (ALA Scientific) using 5 µm carbon fiber electrodes polarized to 650 mV (Chow and von Rüden, 1995; Han et al., 2004). Cells were bathed in a solution containing 150 mM NaCl, 4.2 mM KCl, 1 mM NaH_2PO_4, 0.7 mM $MgCl_2$, 2 mM $CaCl_2$, and 10 mM Hepes, pH 7.4. Secretion was evoked using a Picospritzer (General Valve Corp.) to eject a solution similar to the bathing solution but with 105 mM KCl and 5 mM NaCl.

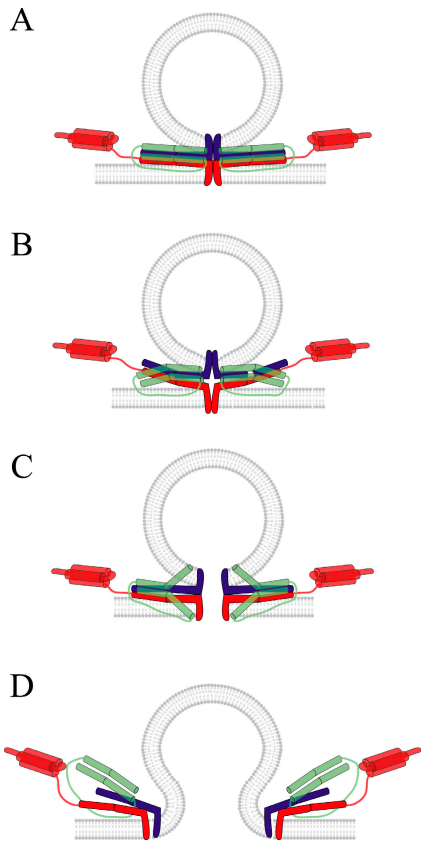

Figure 10. **A model for SNARE-mediated membrane fusion with Syx, Syb, and SNAP-25.** Syx, red; Syb, blue; SNAP-25, green. (A) An initial assembly step leads to an arrangement of SNARE complexes around a contact between the vesicle and plasma membranes. (B) A structural rearrangement in the SNARE complex leads to the formation of a closed fusion pore. (C) The open fusion pore is associated with a partially disassembled SNARE complex. (D) Expansion of the fusion pore is accompanied by further conformational changes in the SNARE complex.

Amperometry spikes were analyzed with the aid of a computer program written in our laboratory by P. Chang (University of Wisconsin, Madison, WI). Cumulative spike counts were based on spikes with peak amplitudes ≥2 pA (~10× the baseline root mean square noise) and were plotted versus time at intervals of 250 ms. PSF were measured for spikes with amplitudes from 20 to 100 pA. The PSF parameters were extracted based on the criteria of Chow and von Rüden (1995). For the determination of mean PSF duration, values were combined across cells, as this quantity shows no significant cell/recording dependence (Wang et al., 2006). PSF lifetimes were sorted into 0.25-ms bins, and the distributions were fitted to a single exponential with Origin software (Microcal). The means obtained in this way were indistinguishable from the arithmetic mean after correction for missed events. The standard errors from these fits were identical to those obtained from a calculation of the arithmetic mean (Colquhoun and Sigworth, 1995). Measurements of kinetic parameters were stable during the course of these studies. For example, dividing our wild-type Syx data on PSF duration into two groups from a 3-yr period gave 0.97 ± 0.06 ms (n = 355) for the first half of the study and 1.06 ± 0.15 ms (n = 204) for the second half.

Cell culture

PC12 cells were cultured as previously described (Hay and Martin, 1992) and transfected using an electroporator (ECM 830; BTX). The pIRES2-EGFP vector (CLONTECH Laboratories, Inc.) was used to overexpress proteins of interest. GFP fluorescence identified cells that were successfully transfected (efficiency of ~30%). A previous study has shown that the overexpression of Syx mutants in this system generally produced levels of protein in transfected cells that exceed the levels of the endogenous protein by ~10-fold (Han et al., 2004). Cells were transferred to dishes coated with collagen I and poly-D-lysine (BD Biosciences) and loaded with 1.5 mM norepinephrine and 0.5 mM ascorbate 14–16 h before experiments. Amperometry was performed 48–96 h after transfection. We note that growing cells in collagen I and poly-D-lysine–coated dishes improved cell adherence and altered secretion. Cells cultured in these coated dishes produced ~50% more spikes and had briefer PSF durations (see Results). Every transfection with mutants was performed together with a transfection of the wild-type protein, and both mutant and wild type were studied in parallel.

Plasmid construction and mutagenesis

Wild-type proteins were subcloned into the pIRES2-EGFP vector using pairs of restriction enzymes. Single and double point mutations were generated using QuikChange site-directed mutagenesis PCR (Stratagene). Syx was truncated by removal of the membrane anchor 23 amino acids from I266 (ΔTM) or the NH_2-terminal H_{abc} domain to I186 (ΔH_{abc}). The Syx-linker construct (provided by J. Rothman, Columbia University, New York, NY) contains 11 extra amino acids with a sequence of LGGSGGSGGSK between K265 and I266L (McNew et al., 1999). NSF and α-SNAP were provided by P. Hanson (Washington University, St. Louis, MO; Hanson et al., 1997; Marz et al., 2003). All constructs were subcloned into the pIRES2-EGFP vector and verified by sequencing.

Statistics

Rates of secretion were determined for individual cells and averaged. Standard errors for the initial and sustained rates and for PSF amplitudes were calculated using the number of cells, recognizing that cell-to-cell variation is the principle source of error in such measurements (Colliver et al., 2000). Statistical analysis was performed with Instat for one-way ANOVA and Prism (GraphPad Software, Inc.) for two-way ANOVA. One-way ANOVA was applied to groups of measurements displayed together in the panels of figures presented in this study. When this test rejected the hypothesis that all of the measurements within that group had the same mean, Dunnett's post-test was used to identify measurements from mutants that differed from the wild-type protein. Because Dunnett's test is conservative, we also applied the t test, and, in five cases, this test detected significant changes when Dunnett's test failed. These are mentioned in the text. We note that this is a reasonable number of uncertain cases of statistical significance for >100 evaluations performed in this study on different rate processes.

Two-way ANOVA was used to examine differences between SNARE mutation effects on the sustained rate and the initial rate. Mutations within the same SNARE helix were grouped, and influences on the initial rate and the sustained rate were evaluated. First, two-way ANOVA tested for an interaction of effects of mutations on the initial and sustained rates. In other words, this test evaluated correlations between the two rate parameters among the different mutations. When this test indicated no interaction between the initial and sustained rates (i.e., the changes were correlated), a second application of two-way ANOVA was made to test whether the variation could be attributed to mutation dependence or rate dependence. Mutation dependence has important implications, as it suggests that some residues have a greater influence on one rate process than on the other.

Online supplemental material

The first part of the online supplemental data presents Ca^{2+} current data that was obtained with the whole-cell patch-clamp. Fig. S1 shows that the Ca^{2+} currents were identical in cells transfected with wild-type protein and selected mutants. The second part of the online data examines protein localization. Fig. S2 presents fluorescence immunostaining that shows that the overexpressed wild-type and mutant proteins are found in the correct places. Syx, SNAP-25, and selected mutants of these proteins appear on the edges of cells; Syb and a mutation show a punctal appearance and colocalize with synaptotagmin. Fig. S3 shows linear regression analysis of kinetic parameters versus the SNARE complex melting temperature to make the point that the kinetic perturbations are not correlated with the stability of SNARE complexes in vitro. Online supplemental material is available at http://www.jcb.org/cgi/content/full/jcb.200510012/DC1.

We thank Payne Chang, Zhenjie Zhang, Zhen Zhang, and Ed Chapman for helpful discussions and critical comments on the manuscript and Payne Chang for ongoing development of the software. We thank Min Dong, Camin Dean, Mike Chika, Akhil Bhalla, and Ed Chapman for valuable advice, assistance, and reagents for the immunocytochemical analysis of localization.

This research was supported by National Institutes of Health grants NS44057 and NS30016.

Submitted: 4 October 2005
Accepted: 7 December 2005

References

Augustine, G.J., M.E. Burns, W.M. DeBello, S. Hilfiker, J.R. Morgan, F.E. Schweizer, H. Tokumaru, and K. Umayahara. 1999. Proteins involved in synaptic vesicle trafficking. *J. Physiol.* 520:33–41.

Bai, J., C.T. Wang, D.A. Richards, M.B. Jackson, and E.R. Chapman. 2004. Fusion pore dynamics are regulated by synaptotagmin*t-SNARE interactions. *Neuron*. 41:929–942.

Bezprozvanny, I., P. Zhong, R.H. Scheller, and R.W. Tsien. 2000. Molecular determinants of the functional interaction between syntaxin and N-type Ca2+ channel gating. *Proc. Natl. Acad. Sci. USA*. 97:13943–13948.

Borisovska, M., Y. Zhao, Y. Tsytsyura, N. Glyvuk, S. Takamori, U. Matti, J. Rettig, T. Sudhof, and D. Bruns. 2005. v-SNAREs control exocytosis of vesicles from priming to fusion. *EMBO J*. 24:2114–2126.

Broadie, K., A. Prokop, H.J. Bellen, C.J. O'Kane, K.L. Schulze, and S.T. Sweeney. 1995. Syntaxin and synaptobrevin function downstream of vesicle docking in *Drosophila*. *Neuron*. 15:663–673.

Chen, Y.A., S.J. Scales, S.M. Patel, Y.C. Doung, and R.H. Scheller. 1999. SNARE complex formation is triggered by Ca2+ and drives membrane fusion. *Cell*. 97:165–174.

Chow, R.H., and L. von Rüden. 1995. Electrochemical detection of secretion from single cells. *In* Single-Channel Recording. B. Sakmann and E. Neher, editors. Plenum Press, New York. 245–275.

Chow, R.H., L. von Rüden, and E. Neher. 1992. Delay in vesicle fusion revealed by electrochemical monitoring of single secretory events in adrenal chromaffin cells. *Nature*. 356:60–63.

Colliver, T.L., E.J. Hess, E.N. Pothos, D. Sulzer, and A.G. Ewing. 2000. Quantitative and statistical analysis of the shape of amperometric spikes recorded from two populations of cells. *J. Neurochem.* 74:1086–1097.

Colquhoun, D., and F. Sigworth. 1995. Fitting and statistical analysis of single channel records. *In* Single-Channel Recording. B. Sakmann and E. Neher, editors. Plenum, New York. 483–587.

Deak, F., S. Schoch, X. Liu, T.C. Sudhof, and E.T. Kavalali. 2004. Synaptobrevin is essential for fast synaptic-vesicle endocytosis. *Nat. Cell Biol.* 6:1102–1108.

Dulubova, I., S. Sugita, S. Hill, M. Hosaka, I. Fernandez, T.C. Sudhof, and J. Rizo. 1999. A conformational switch in syntaxin during exocytosis: role of munc18. *EMBO J.* 18:4372–4382.

Fasshauer, D. 2003. Structural insights into the SNARE mechanism. *Biochim. Biophys. Acta*. 1641:87–97.

Fasshauer, D., W.K. Eliason, A.T. Brunger, and R. Jahn. 1998. Identification of a minimal core of the synaptic SNARE complex sufficient for reversible assembly and disassembly. *Biochemistry*. 37:10354–10362.

Fasshauer, D., W. Antonin, V. Subramaniam, and R. Jahn. 2002. SNARE assembly and disassembly exhibit a pronounced hysteresis. *Nat. Struct. Biol.* 9:144–151.

Fergestad, T., M.N. Wu, K.L. Schulze, T.E. Lloyd, H.J. Bellen, and K. Broadie. 2001. Targeted mutations in the syntaxin H3 domain specifically disrupt SNARE complex function in synaptic transmission. *J. Neurosci.* 21:9142–9150.

Fiebig, K.M., L.M. Rice, E. Pollock, and A.T. Brunger. 1999. Folding intermediates of SNARE complex assembly. *Nat. Struct. Biol.* 6:117–123.

Finley, M.F., S.M. Patel, D.V. Madison, and R.H. Scheller. 2002. The core membrane fusion complex governs the probability of synaptic vesicle fusion but not transmitter release kinetics. *J. Neurosci.* 22:1266–1272.

Gong, L.W., G. Di Paolo, E. Diaz, G. Cestra, M.E. Diaz, M. Lindau, P. De Camilli, and D. Toomre. 2005. Phosphatidylinositol phosphate kinase type I gamma regulates dynamics of large dense-core vesicle fusion. *Proc. Natl. Acad. Sci. USA*. 102:5204–5209.

Graham, M.E., J.W. Barclay, and R.D. Burgoyne. 2004. Syntaxin/Munc18 interactions in the late events during vesicle fusion and release in exocytosis. *J. Biol. Chem.* 279:32751–32760.

Grote, E., J.C. Hao, M.K. Bennett, and R.B. Kelly. 1995. A targeting signal in VAMP regulating transport to synaptic vesicles. *Cell*. 81:581–589.

Han, X., and M.B. Jackson. 2005. Electrostatic interactions between the syntaxin membrane anchor and neurotransmitter passing through the fusion pore. *Biophys. J.* 88:L20–L22.

Han, X., C.T. Wang, J. Bai, E.R. Chapman, and M.B. Jackson. 2004. Transmembrane segments of syntaxin line the fusion pore of Ca2+-triggered exocytosis. *Science*. 304:289–292.

Hanson, P.I., R. Roth, H. Morisaki, R. Jahn, and J.E. Heuser. 1997. Structure and conformational changes in NSF and its membrane receptor complexes visualized by quick-freeze/deep-etch electron microscopy. *Cell*. 90:523–535.

Hao, J.C., N. Salem, X.R. Peng, R.B. Kelly, and M.K. Bennett. 1997. Effect of mutations in vesicle-associated membrane protein (VAMP) on the assembly of multimeric protein complexes. *J. Neurosci.* 17:1596–1603.

Hata, Y., C.A. Slaughter, and T.C. Sudhof. 1993. Synaptic vesicle fusion complex contains unc-18 homologue bound to syntaxin. *Nature*. 366:347–351.

Hay, J.C., and T.F. Martin. 1992. Resolution of regulated secretion into sequential MgATP-dependent and calcium-dependent stages mediated by distinct cytosolic proteins. *J. Cell Biol.* 119:139–151.

Hayashi, T., H. McMahon, S. Yamasaki, T. Binz, Y. Hata, T.C. Sudhof, and H. Niemann. 1994. Synaptic vesicle membrane fusion complex: action of clostridial neurotoxins on assembly. *EMBO J.* 13:5051–5061.

Hayashi, T., S. Yamasaki, S. Nauenburg, T. Binz, and H. Niemann. 1995. Disassembly of the reconstituted synaptic vesicle membrane fusion complex in vitro. *EMBO J.* 14:2317–2325.

Heinemann, C., R.H. Chow, E. Neher, and R.S. Zucker. 1994. Kinetics of the secretory response in bovine chromaffin cells following flash photolysis of caged Ca^{2+}. *Biophys. J.* 67:2546–2557.

Hua, S.Y., and M.P. Charlton. 1999. Activity-dependent changes in partial VAMP complexes during neurotransmitter release. *Nat. Neurosci.* 2:1078–1083.

Jahn, R., and T.C. Sudhof. 1999. Membrane fusion and exocytosis. *Annu. Rev. Biochem.* 68:863–911.

Jahn, R., P.I. Hanson, H. Otto, and G. Ahnert-Hilger. 1995. Botulinum and tetanus neurotoxins: emerging tools for the study of membrane fusion. *Cold Spring Harb. Symp. Quant. Biol.* 60:329–335.

Kee, Y., R.C. Lin, S.C. Hsu, and R.H. Scheller. 1995. Distinct domains of syntaxin are required for synaptic vesicle fusion complex formation and dissociation. *Neuron*. 14:991–998.

Lin, R.C., and R.H. Scheller. 1997. Structural organization of the synaptic exocytosis core complex. *Neuron*. 19:1087–1094.

Lin, R.C., and R.H. Scheller. 2000. Mechanisms of synaptic vesicle exocytosis. *Annu. Rev. Cell Dev. Biol.* 16:19–49.

Littleton, J.T., E.R. Chapman, R. Kreber, M.B. Garment, S.D. Carlson, and B. Ganetzky. 1998. Temperature-sensitive paralytic mutations demonstrate that synaptic exocytosis requires SNARE complex assembly and disassembly. *Neuron*. 21:401–413.

Lou, X., V. Scheuss, and R. Schneggenburger. 2005. Allosteric modulation of the presynaptic Ca2+ sensor for vesicle fusion. *Nature*. 435:497–501.

Marz, K.E., J.M. Lauer, and P.I. Hanson. 2003. Defining the SNARE complex binding surface of alpha-SNAP: implications for SNARE complex disassembly. *J. Biol. Chem.* 278:27000–27008.

McNew, J.A., T. Weber, D.M. Engelman, T.H. Sollner, and J.E. Rothman. 1999. The length of the flexible SNAREpin juxtamembrane region is a critical determinant of SNARE-dependent fusion. *Mol. Cell*. 4:415–421.

Melia, T.J., T. Weber, J.A. McNew, L.E. Fisher, R.J. Johnston, F. Parlati, L.K. Mahal, T.H. Sollner, and J.E. Rothman. 2002. Regulation of membrane fusion by the membrane-proximal coil of the t-SNARE during zippering of SNAREpins. *J. Cell Biol.* 158:929–940.

Misura, K.M., R.H. Scheller, and W.I. Weis. 2000. Three-dimensional structure of the neuronal-Sec1-syntaxin 1a complex. *Nature*. 404:355–362.

Pevsner, J., S.C. Hsu, and R.H. Scheller. 1994. n-Sec1: a neural-specific syntaxin-binding protein. *Proc. Natl. Acad. Sci. USA*. 91:1445–1449.

Poirier, M.A., W. Xiao, J.C. Macosko, C. Chan, Y.K. Shin, and M.K. Bennett. 1998. The synaptic SNARE complex is a parallel four-stranded helical bundle. *Nat. Struct. Biol.* 5:765–769.

Rossi, G., A. Salminen, L.M. Rice, A.T. Brunger, and P. Brennwald. 1997. Analysis of a yeast SNARE complex reveals remarkable similarity to the neuronal SNARE complex and a novel function for the C terminus of the SNAP-25 homolog, Sec9. *J. Biol. Chem.* 272:16610–16617.

Schiavo, G., M. Matteoli, and C. Montecucco. 2000. Neurotoxins affecting neuroexocytosis. *Physiol. Rev.* 80:717–766.

Schoch, S., F. Deak, A. Konigstorfer, M. Mozhayeva, Y. Sara, T.C. Sudhof, and E.T. Kavalali. 2001. SNARE function analyzed in synaptobrevin/VAMP knockout mice. *Science*. 294:1117–1122.

Schulze, K.L., K. Broadie, M.S. Perin, and H.J. Bellen. 1995. Genetic and electrophysiological studies of *Drosophila* syntaxin-1A demonstrate its role in nonneuronal secretion and neurotransmission. *Cell*. 80:311–320.

Schweizer, F.E., T. Dresbach, W.M. DeBello, V. O'Connor, G.J. Augustine, and H. Betz. 1998. Regulation of neurotransmitter release kinetics by NSF. *Science*. 279:1203–1206.

Sollner, T., M.K. Bennett, S.W. Whiteheart, R.H. Scheller, and J.E. Rothman. 1993a. A protein assembly disassembly pathway in vitro that may correspond to sequential steps of synaptic vesicle docking, activation, and fusion. *Cell*. 75:409–418.

Sollner, T., S.W. Whiteheart, M. Brunner, H. Erdjument-Bromage, S. Geromanos, P. Tempst, and J.E. Rothman. 1993b. SNAP receptors implicated in vesicle targeting and fusion. *Nature*. 362:318–324.

Sorensen, J.B., G. Nagy, F. Varoqueaux, R.B. Nehring, N. Brose, M.C. Wilson, and E. Neher. 2003. Differential control of the releasable vesicle pools by SNAP-25 splice variants and SNAP-23. *Cell*. 114:75–86.

Sutton, R.B., D. Fasshauer, R. Jahn, and A.T. Brunger. 1998. Crystal structure of a SNARE complex involved in synaptic exocytosis at 2.4 angstrom resolution. *Nature*. 395:347–353.

Tucker, W.C., J.M. Edwardson, J. Bai, H.J. Kim, T.F. Martin, and E.R. Chapman. 2003. Identification of synaptotagmin effectors via acute inhibition of secretion from cracked PC12 cells. *J. Cell Biol.* 162:199–209.

Tucker, W.C., T. Weber, and E.R. Chapman. 2004. Reconstitution of Ca2+-regulated membrane fusion by synaptotagmin and SNAREs. *Science*. 304:435–438.

Voets, T., E. Neher, and T. Moser. 1999. Mechanisms underlying phasic and sustained secretion in chromaffin cells from mouse adrenal slices. *Neuron*. 23:607–615.

Wang, C.-T., R. Grishanin, C.A. Earles, P.Y. Chang, T.F.J. Martin, E.R. Chapman, and M.B. Jackson. 2001. Synaptotagmin modulation of fusion pore kinetics in regulated exocytosis of dense-core vesicles. *Science*. 294:1111–1115.

Wang, C.-T., J. Bai, P.Y. Chang, E.R. Chapman, and M.B. Jackson. 2005. Synaptotagmin-Ca^{2+} triggers two sequential steps in regulated exocytosis in rat PC12 cells: fusion pore opening and fusion pore dilation. *J. Physiol.* doi:10.1113/jphysiol.2005.097378.

Washbourne, P., P.M. Thompson, M. Carta, E.T. Costa, J.R. Mathews, G. Lopez-Bendito, Z. Molnar, M.W. Becher, C.F. Valenzuela, L.D. Partridge, and M.C. Wilson. 2002. Genetic ablation of the t-SNARE SNAP-25 distinguishes mechanisms of neuroexocytosis. *Nat. Neurosci.* 5:19–26.

Weber, T., B.V. Zemelman, J.A. McNew, B. Westermann, M. Gmachl, F. Parlati, T.H. Sollner, and J.E. Rothman. 1998. SNAREpins: minimal machinery for membrane fusion. *Cell*. 92:759–772.

Wei, S., T. Xu, U. Ashery, A. Kollewe, U. Matti, W. Antonin, J. Rettig, and E. Neher. 2000. Exocytotic mechanism studied by truncated and zero layer mutants of the C-terminus of SNAP-25. *EMBO J.* 19:1279–1289.

Wu, M.N., T. Fergestad, T.E. Lloyd, Y.C. He, K. Broadie, and H.J. Bellen. 1999. Syntaxin 1A interacts with multiple exocytic proteins to regulate neurotransmitter release in vivo. *Neuron*. 23:593–605.

Xu, T., T. Binz, H. Niemann, and E. Neher. 1998. Multiple kinetic components of exocytosis distinguished by neurotoxin sensitivity. *Nat. Neurosci.* 1:192–200.

Xu, T., B. Rammner, M. Margittai, A.R. Artalejo, E. Neher, and R. Jahn. 1999. Inhibition of SNARE complex assembly differentially affects kinetic components of exocytosis. *Cell*. 99:713–722.

Yang, B., M. Steegmaier, L.C. Gonzalez Jr., and R.H. Scheller. 2000. nSec1 binds a closed conformation of syntaxin1A. *J. Cell Biol.* 148:247–252.

Zhang, F., Y. Chen, Z. Su, and Y.K. Shin. 2004. SNARE assembly and membrane fusion: a kinetic analysis. *J. Biol. Chem.* 279:38668–38672.

Zhou, Z., S. Misler, and R.H. Chow. 1996. Rapid fluctuations in transmitter release from single vesicles in bovine adrenal chromaffin cells. *Biophys. J.* 70:1543–1552.